AGU PUBLICATIONS

JGR

Journal of Geophysical Research: Biogeosciences

RESEARCH ARTICLE
10.1002/2016JG003390

Key Points:
- POM compositions are related to free living than to the particle-attached bacterial community composition
- Particle microniche properties might be important in shaping particle-attached community structure
- Release of DOC from particles significantly influences the free-living bacterial community composition

Supporting Information:
- Supporting Information S1

Correspondence to:
Y. Zhang and N. Jiao,
yaozhang@xmu.edu.cn;
jiao@xmu.edu.cn

Citation:
Zhang, Y., W. Xiao, and N. Jiao (2016), Linking biochemical properties of particles to particle-attached and free-living bacterial community structure along the particle density gradient from freshwater to open ocean, *J. Geophys. Res. Biogeosci.*, *121*, 2261–2274, doi:10.1002/2016JG003390.

Received 24 FEB 2016
Accepted 4 AUG 2016
Accepted article online 10 AUG 2016
Published online 31 AUG 2016

Linking biochemical properties of particles to particle-attached and free-living bacterial community structure along the particle density gradient from freshwater to open ocean

Yao Zhang[1], Wei Xiao[1], and Nianzhi Jiao[1]

[1]State Key Laboratory of Marine Environmental Science and Institute of Marine Microbes and Ecospheres, Xiamen University, Xiamen, China

Abstract To test the hypothesis that particle composition has a stronger influence on the community structure of particle-attached than free-living bacteria, elemental (C/N, δ^{13}C, and δ^{15}N) and chemical composition of particles and the size-fractionated bacterial community composition were examined along the particle density gradient from the Pearl River to the open basin in the South China Sea. Microbial communities were collected at the three size fractions of 0.2–0.8, 0.8–3, and >3 μm, and the community composition was analyzed using high-throughput sequencing of the 16S rRNA gene (V3–V4 regions). Multivariate analysis evaluating the similarities of bacterial community composition and chemical composition of particles revealed their general consistent spatial variations along the particle density gradient from freshwater to the sea basin. However, compositions of particulate organic matter were more strongly related to the free living than to the particle-attached bacterial community composition, which was composed of relatively abundant anaerobic bacteria and those taxa preferring low-oxygen conditions. This latter result might be caused by low-oxygen microzones in particles. Community network models further revealed tighter interactions within the particle-attached than in free-living bacterial communities, suggesting that a relatively confined space in particles is more favorable for interactions within the community. These analyses indicated that particle microniche properties might be important in shaping particle-attached community structure. In contrast, particulate organic matter compositions significantly influenced the free-living bacterial community probably through the release of labile or semilabile organic matter from particles contributing to the bioavailability of dissolved organic carbon.

1. Introduction

Particulate organic matter (POM) is universally important in aquatic ecosystems for organic matter remineralization and elemental cycling [*Simon et al.*, 2014]. Marine particles are generally considered to be organic-rich detrital matter, while estuarine particles tend to be smaller and have significant content of inorganic material [*Sherwood et al.*, 1984]. Most of the previous studies have focused on bulk parameters characterizing POM, such as the carbon (C) and nitrogen (N) content, C/N ratio, and chlorophyll concentrations [*Çoban-Yıldız et al.*, 2006a; *Kao et al.*, 2012; *Huang et al.*, 2010]. However, the molecular composition of POM as determined by mass spectrometry is not well understood. Marine bacteria can respond to organic particles in sea water through dense colonization and metabolic activities [*Ganesh et al.*, 2014], creating hotspots of bacterial growth and carbon cycling [*Azam and Long*, 2001]. Further, marine bacteria concurrently shape the nature and quantity of organic C and N [*D'Ambrosio et al.*, 2014]. Thus, the composition of POM is likely to be closely related to the attached bacterial taxa and biochemical processes and characterization of POM in different ecosystems is essential to understand this linkage.

Microorganisms colonize and remineralize organic particles, which in turn can lead to a dissolved organic carbon (DOC) plume surrounding the particles [*Grossart*, 2010; *Stocker*, 2012]. This means that particles, as direct substrates, could select for the corresponding particle-attached bacterial community structure and function, while the DOC plume from particles could select for the free-living bacterial community. The composition of particle-attached bacterial communities compared with their free-living counterparts has been investigated in many aquatic ecosystems [*Crump et al.*, 1999; *Delong et al.*, 1993; *Ghiglione et al.*, 2007; *Zhang et al.*, 2007]. However, these studies have not demonstrated a consistent trend in community

composition. Many factors, such as particle residence times and geographic location [*Fuhrman et al*., 2008], particle sources and substrate availability [*Grossart*, 2010], and nutrient gradients [*Carlson et al*., 2008], can affect particle-attached and free-living bacterial communities. Particle composition is likely to have the most direct influence on their attached bacteria. Thus, we hypothesize that particles have a stronger influence on particle-attached than free-living bacterial communities. However, very few studies have addressed the relationship between particle composition and microbes [*Edwards et al*., 2015]. The molecular characterization of particle-attached microbiota and free-living counterparts would help to reveal specific details about the mechanisms regulating fluxes of particulate organic carbon (POC) to DOC, which will ultimately influence the rates of carbon export and storage [*Jiao et al*., 2010, 2014].

To investigate the relationship between particle composition and particle-attached and free-living bacterial communities, a gradient from particle-rich to particle-poor water is necessary to help reveal patterns and mechanisms. The South China Sea (SCS) is a marginal sea in the Northwest Pacific. With large amounts of particle-rich freshwater and terrigenous input from the Pearl River and particle-poor oceanic water intruding into the continental shelf, the SCS is characterized by a sharp gradient in particle concentration over a small spatial region [*Ning et al*., 2004]. These features make the SCS an ideal environment for examining the relationship between particles and microbes. In the present study, the bacterial community composition in three size fractions (0.2–0.8, 0.8–3, and >3 μm) and particle composition including stable isotope composition, C/N ratio, and chemical composition were analyzed along the particle density gradient from the Pearl River to the open basin in the SCS. The objectives of this study were to (1) compare bacterial community composition in different size fractions and their relationships with particle composition among different water masses; (2) test whether particle composition was more closely related to particle-attached than free-living bacterial community composition; and (3) if not, which factors should be considered in shaping particle-attached and free-living bacterial communities.

2. Materials and Methods

2.1. Study Site and Sampling

A total of 21 sites covering the Pearl River, the estuary, the continental shelf, and the basin area were sampled in the SCS (Figure 1a) during two cruises from 27 to 31 July 2013 and from 20 September 2013 to 23 October 2013. In total, 18 samples were collected from the surface and bottom of the freshwater station (R1, 9 m depth), estuarine station (E1, 9 m depth), and continental shelf stations (S1–S7, 45–131 m depth); and 12 samples were collected from surface water of the sea basin stations (B1–B12, >543 m depth). Water samples were collected using a submersible pump at R1 and E1 and a conductivity-temperature-depth (CTD)-rosette sampling system with 6 L Go-Flo bottles (SBE 9/17 plus, SeaBird Inc., USA) at S1–S7 and B1–B12. For gene analysis, 200 mL to 6 L samples were first filtered through a 20 μm NYTEX net (at the R1 and E1 sites) and then through 3, 0.8, and 0.2 μm pore-size polycarbonate filters (47 mm diameter; Millipore) at a pressure of <0.03 MPa to collect the three size fractions. Filtered samples were flash frozen in liquid nitrogen and subsequently stored at −80°C until DNA extraction. For particulate matter analysis, 20 mL to 20 L samples were collected on precombusted (450°C for 4 h) 0.7 μm pore-size GF/F filters (47 mm diameter; Whatman). Filters were placed in petri dishes and immediately stored at −20°C until further analysis; seawater was collected in precombusted (500°C for 6 h) 40 mL glass vials and immediately stored at −20°C for DOC analysis. For total chlorophyll *a* (Chl *a*) analysis, 500 mL seawater was filtered through 0.7 μm pore-size GF/F filters (47 mm diameter; Whatman). Filtered samples were flash frozen in liquid nitrogen and subsequently transferred to −80°C in the laboratory until further analysis.

2.2. Particulate Material Analysis

Filters with particulate material were freeze dried for 24 h. Carbonate was removed by fuming with concentrated HCl vapor for 48 h and then the filters were washed with Milli-Q water. All filters were dried at 60°C to a constant weight and then stored in sealed petri dishes prior to isotopic analysis. Particulate organic C, organic N (PON), and their isotopic composition (δ^{13}C-POC and δ^{15}N-PON) were analyzed using a continuous-flow elemental analyzer (Flash EA 1112 HT) coupled to an isotope ratio mass spectrometer (Thermo Finnigan Delta V Advantage) system. Helium was used as a carrier gas at a flow rate of 90 mL min^{-1}. The temperature of the reaction column and chromatographic column were 960°C and 50°C, respectively. The C and N

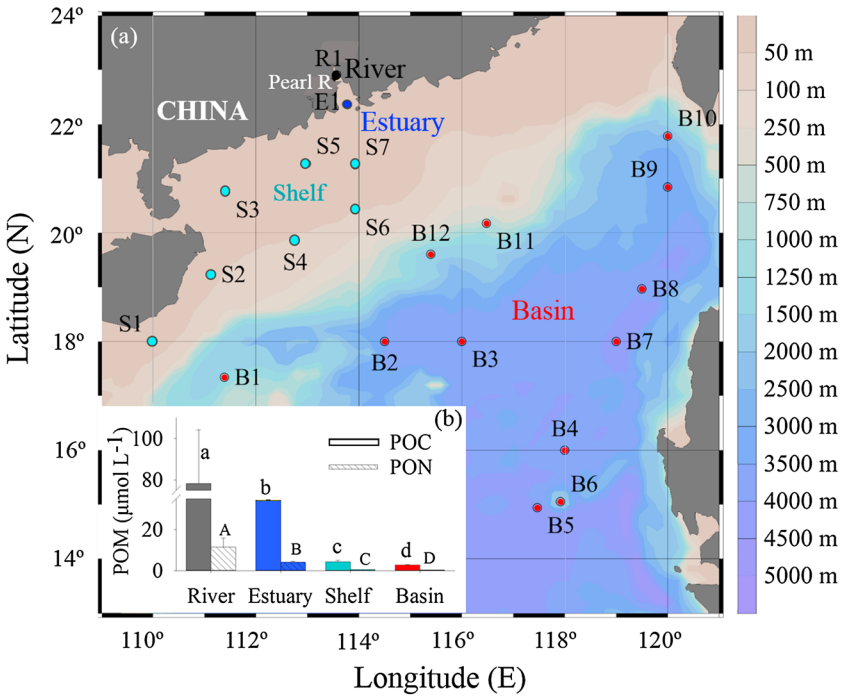

Figure 1. (a) Map of the South China Sea (SCS) showing sampling stations. Black circle, the river station; dark blue circle, the estuary station; light blue circles, the continental shelf stations; red circles, the sea basin stations. Consistent colors were used throughout. Isobaths are used as the background and the color bar indicates depth. (b) POC and PON concentrations along the particle density gradient from freshwater to the sea basin. Significant differences ($P < 0.05$) in POC and PON concentrations among the different regions were indicated by different lowercase letters and capital letters, respectively.

isotopic ratios ($^{13}C/^{12}C$ and $^{15}N/^{14}N$) were calibrated to working standards and are presented by δ notion (units of per mil (‰)):

$$\delta(‰) = \left[\left(R_{\text{sample}}/R_{\text{reference}}\right) - 1\right] \times 1000 \quad (1)$$

where R_{sample} and $R_{\text{reference}}$ indicate the ^{13}C:^{12}C or ^{15}N:^{14}N isotopic ratios of the sample and standard, respectively. Vienna PeeDee Belemnite and atmospheric N_2 were used as the international reference materials for C and N, respectively, and the analytical precision of this method was 0.2‰ for $\delta^{13}C$ and 0.25‰ for $\delta^{13}C$. High-performance liquid chromatography was used to measure total Chl *a* concentration according to the protocol of *Huang et al*. [2010].

The chemical composition of POM was analyzed with pyrolysis-gas chromatography-mass spectrometry as described by *Çoban-Yıldız et al*. [2006b]. First, particulate matter on filters was carefully scraped to collect about 6 mg in a quartz tube and was then moistened with 100 μL of tetramethylammonium hydroxide (25% in methanol) solution. The ends of the tube were loosely plugged with prepyrolyzed quartz wool, and samples were pyrolyzed at 550°C using a single point pyrolyzer (Frontier Laboratories Ltd., Japan) interfaced directly to a gas chromatography/mass spectrometry (QP2010, Shimadzu, Japan). The pyrolysis product was automatically injected into the gas chromatograph. Helium was used as a carrier gas at a flow rate of 1.8 mL min^{-1}. The column temperature was set at 40°C for 3 min and then increased at a rate of 10°C min^{-1} to 300°C for 15 min. The mass spectrometer was operated at an ionization energy of 70 eV (EI) with a mass detection range (*m/z*) of 25–500 and a cycle time of 1 s. Pyrolysis products were quantified by peak height, and compounds were identified by comparing the obtained mass spectra with the National Institute of Standards and Technology Mass Spectral Library database, published spectra, and real standards.

2.3. Other Biogeochemical Analyses

Temperature, salinity, and water depth were measured using a Horiba instrument (Model W-20XD, Kyoto, Japan) or a CTD system (SBE 911plus; SeaBird, Washington, USA). DOC was measured using a Shimadzu TOC-V analyzer; the detailed procedure was described in *Wu et al*. [2015].

2.4. DNA Extraction, Polymerase Chain Reaction (PCR), Sequencing, and Sequence Analysis

DNA extraction was performed according to the phenol-chloroform-isoamyl alcohol method [*Massana et al*., 2000]. The quality and quantity of DNA were assessed with a NanoDrop device (ND-2000; Thermo Fisher) and stored at −80°C until use. The bacterial hypervariable regions V3–V4 of 16S rRNA genes were amplified using the primers 341F (5′-CCTAYGGGRBGCASCAG-3′) and 806R (5′-GGACTACNNGGGTATCTAAT-3′), with a unique barcode sequence at the 5′ end. PCR reactions were performed in 30 μL reactions with 5–100 ng of DNA template. Reaction conditions consisted of an initial denaturation at 98°C for 1 min, followed by 30 cycles of denaturation at 98°C for 10 s, annealing at 50°C for 30 s, and elongation at 72°C for 30 s, with a final extension at 72°C for 5 min. Equimolar amounts of PCR amplicons from different samples were mixed and purified with the GeneJET Gel Extraction Kit (Thermo Scientific). Sequencing libraries were generated using the NEB Next® Ultra™ DNA Library Prep Kit for Illumina (NEB, USA) following the manufacturer's recommendations. The quality of the libraries was assessed with a Qubit 2.0 Fluorometer (Thermo Scientific) and Agilent Bioanalyzer 2100 system. Finally, the library was sequenced on an Illumina MiSeq platform, and 250 bp paired-end reads were generated.

Paired-end reads from the original DNA fragments were merged by using FLASH (Fast Length Adjustment of SHort reads) software [*Magoč and Salzberg*, 2011]. The criteria previously described [*Sogin et al*., 2006] were used to assess the quality of sequence reads. We eliminated sequences that contained more than one ambiguous nucleotide (N), that did not have a complete barcode and primer at one end, or that were shorter than 200 bp after removal of the barcode and primer sequences. The remaining sequences passing the pipeline filters were assigned to samples by examining the barcode. Quality-controlled sequences were analyzed using MOTHUR following the standard operating procedure (http://www.mothur.org/wiki/MiSeq_SOP) [*Kozich et al*., 2013]. Briefly, sequences were aligned to the SILVA database, and the resulting alignment was then screened and filtered using the *screen.seqs* and *filter.seqs* commands to ensure that all the sequences overlapped in the same alignment space. Sequences within 2 bp difference of a more abundant sequence were merged with the *pre.cluster* command for reducing sequencing errors. Chimeras were removed using the Uchime algorithm in MOTHUR. Finally, classification analyses of sequences were carried out using the Bayesian classifier with the *classify.seqs* command and the confidence cut off was set to 60%. Sequences that were classified as "Cyanobacteria_Chlorolast," or "Mitochondria," or "unknown" (could not be classified at the kingdom level) were removed from the data set. All samples were analyzed at the same sequencing depth using the *sub.sample* command for normalization. Sequences were further clustered into operational taxonomic units (OTUs) using the furthest neighbor algorithm, and the cutoff value was set at 0.03 for the heterotrophic bacterial (noncyanobacterial) assemblage and 0.01 for *Cyanobacteria* [*Zhang et al*., 2014a]. Sample richness and diversity indices (Chao, Simpson, and Shannon) were calculated in MOTHUR. Sequencing data were deposited in the NCBI Sequence Read Archive: SRP068543.

2.5. Statistical Analyses

Nonmetric multidimensional scaling (NMDS) was used to determine the similarity of samples to each other based on Bray-Curtis similarities [*Clarke and Warwick*, 1994] with PRIMER 5 software (Primer-E 2000). Bray-Curtis similarities were calculated based on relative abundance matrices of OTUs for communities or chemical composition for POM. Similarities among the samples were represented in a multidimensional space by putting more similar samples closer together [*Kruskal*, 1964]. Significance tests for differences between samples were performed using the one-way analysis of similarity (ANOSIM) [*Clarke and Warwick*, 1994]. Similarity percentage (SIMPER) analysis in PRIMER was used to identify which organisms were responsible for the similarity and dissimilarity observed in community composition after taxonomy was assigned to each OTU. Canonical correspondence analysis (CCA) was used to further analyze variations in bacterial communities under the constraint of environmental factors (Z transformation) and POM chemistry with CANOCO software [*Ter Braak*, 1989]. An optimal CCA model was produced with "forward selection" via a Monte Carlo permutation test (999 permutations; default setting). Significant explanatory parameters ($P < 0.05$) without multicollinearity (variance inflation factor < 20) [*Ter Braak*, 1986] were obtained for the community structure.

Standard and partial Mantel tests were run in *R* (VEGAN) to determine correlations between environmental factors and POM elementary composition (δ^{13}C, δ^{15}N, and C/N ratio) or POM chemical composition (based on the relative abundance of pyrolysis products) and bacterial community composition (based on the relative abundance of all OTUs). The standard Mantel test estimates the correlation between two matrices, while the

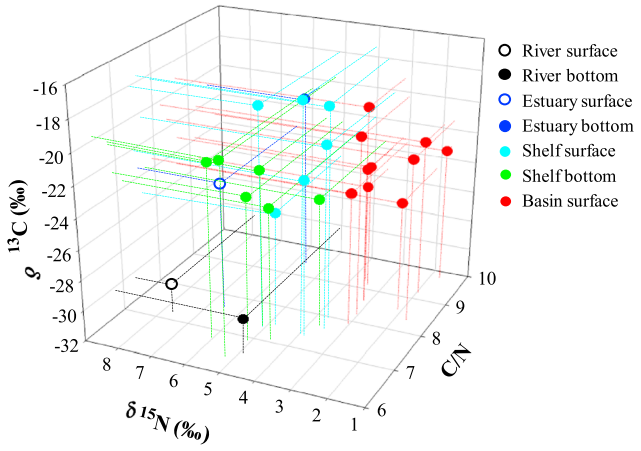

Figure 2. Stable isotopic compositions (δ^{13}C and δ^{15}N) and the C/N ratios of particulate matter in different regions of the SCS.

partial Mantel test estimates the correlation between two matrices, controlling for the effects of a third matrix. Dissimilarity matrices of communities were based on Bray-Curtis distances between samples. Environmental parameters and POM elementary composition were normalized using z-score transformation; POM chemical composition was based on the relative abundance, and Euclidean distances between samples were calculated. The significance of the Mantel statistics based on Pearson's product-moment correlation was obtained after 999 permutations. Mantel tests were performed on data for all samples according to the different size fractions, including samples from the river to the continental shelf and those from the sea basin. The results of the statistical tests were assumed to be significant at P values ≤ 0.05.

2.6. Network Analysis

In an ecosystem, different species/populations interact with each other to form complicated networks through various types of interactions such as predation, competition, and mutualism [*Deng et al*., 2012]. Based on gene abundance data, a network graph can be developed to represent the ecological interactions (links) of different gene markers (nodes) in a microbial community [*Fuhrman et al*., 2008]. Strictly speaking, the ecological networks determined in this way reflected the interactions among different microbial populations carrying the OTUs rather than individual "species" in a microbial community [*Zhou et al*., 2010]. In the present study, potential interactions between bacterial taxa were determined through modeling the microbial community in the network structure.

A general framework of network analysis is processed according to the protocol of *Zhou et al*. [2010]. Only when a community cluster contains more than eight samples/libraries in cluster analysis can it be analyzed as a complete ecological network and its constituent samples/libraries can be used as replicates. First, the data sets were uploaded to the open-accessible network analysis pipeline (Molecular Ecological Network Analysis Pipeline, MENAP, http://ieg2.ou.edu/MENA). A pairwise Pearson correlation between any two genes was estimated based on the gene abundance data to measure their similarity. Then, the obtained similarity matrix was transformed into an adjacency matrix, which measures the strengths of the connections between nodes, by applying a threshold to the correlation values using random matrix theory-based methods. Once the adjacency matrix was defined, module analysis and network characterization were performed. Summing the strengths of the connections of each gene with all of the other connected genes yielded a single network parameter, connectivity, which represents how strongly that gene is connected to all of the other genes in the network [*Zhou et al*., 2010].

In a network graph, each node represents an OTU indicating an individual taxon. The edge (line) between each two nodes represents positive or negative interactions between those two taxa. For instance, negative interactions within bacterial communities hint at competitive interactions and could be explained by competition for the same resource [*Montoya et al*., 2006; *Bascompte*, 2007].

3. Results and Discussion

3.1. Biochemical Properties of Particles

POC and PON concentrations showed a decreasing trend, ranging from 2.13 to 104.11 μM and from 0.26 to 15.76 μM, respectively, along the particle density gradient from freshwater to the SCS basin (Figure 1b). Stable C and N isotopic ratios and C/N ratios (Figure 2) were used to investigate the origins of POM [*Çoban-Yıldız et al*., 2006a; *Kao et al*., 2012; *Kumar et al*., 2011]. The relatively depleted δ^{13}C values of

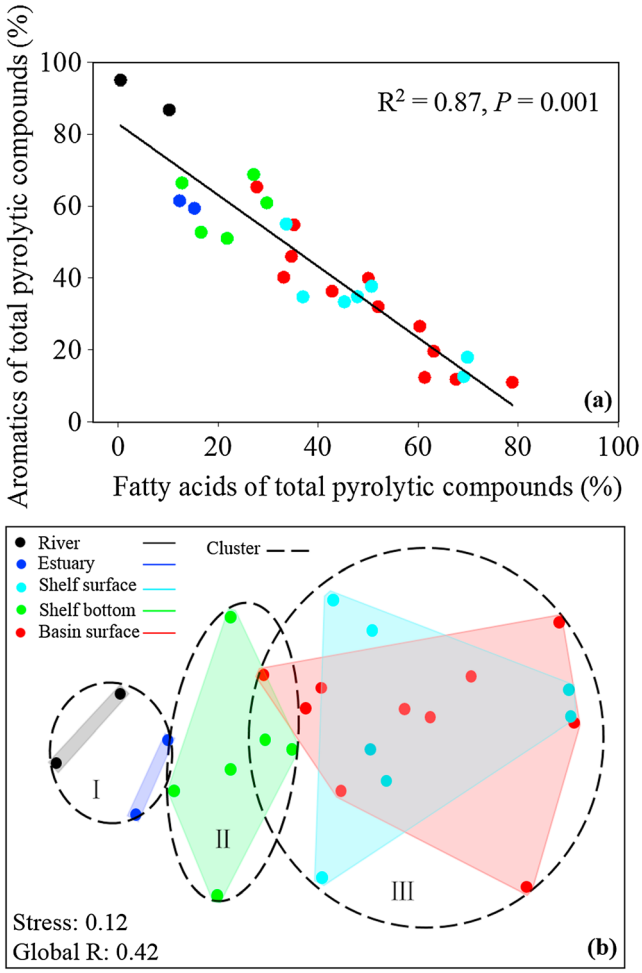

Figure 3. (a) Scatterplot of aromatic and fatty acid compound content of total pyrolytic compounds showing a significant negative correlation between them. (b) Nonmetric multidimensional scaling (NMDS) ordination based on Bray-Curtis similarities between chemical composition profiles of POM. Each circle represents an individual sample in the NMDS charts. Roman numerals represent cluster serial number.

POM at the freshwater station R1 (−30.19‰ to −29.75‰) suggested a dominant contribution of C3 plants and riverine phytoplankton (average: −29.0‰) [*Zhang et al.*, 2014c]. The highest $\delta^{15}N$ value occurred in surface water of site R1 (7.78‰) and gradually decreased from freshwater in an off-shore direction (estuary: 5.82‰–6.42‰; shelf: 3.48‰–6.62‰; basin: 1.68‰–3.60‰). This could be explained by isotopic fractionation during trophic transfer of nitrogenous compounds [*Çoban-Yıldız et al.*, 2006a] and variation in source associated with terrigenous input and various biogeochemial transformations such as denitrification, nitrification, nitrate (NO_3^-) assimilation, and N_2 fixation [*Kumar et al.*, 2011]. Isotopic fractionation by phytoplankton blooms that can cause elevated $\delta^{15}N$ [*Pennock et al.*, 1996] might not be the main reason for this observation. An elevated C/N ratio could be observed when phytoplankton bloom [*Geider and La Roche*, 2002; *Zhao et al.*, 2009]. However, in the present study, the C/N ratios at R1 were similar to those at the estuary and shelf stations (6.36–8.25) and were lower than those at the basin stations (7.91–9.78). The decrease in terrestrial inputs containing N and the increasing contribution of phytoplankton that contain rich oligosaccharide and polysaccharide [*Strom et al.*, 1997] to POM might elevate the C/N ratios in the basin [*Conan et al.*, 2007], although there was a general seaward decrease in total Chl *a* concentration (supporting information Figure S1).

In total, 185 different pyrolytic compounds were recognized in the 27 samples and were classified into six compound classes according to their source and chemical similarity: aromatics, fatty acids, alkanes/alkenes, carbohydrates, phenols, and N compounds. Aromatic and fatty acid compounds contributed a majority of pyrolysis products, and there was a significantly negative correlation ($P < 0.05$) between their distributions along the particle density gradient from freshwater to the sea basin (Figure 3a). Two-dimensional NMDS ordination was performed to evaluate similarities among pyrolytic profiles of POM. Three clusters were formed along the particle density gradient from freshwater to the sea basin: the freshwater-estuary cluster (I); the shelf bottom cluster (II); and the shelf-basin surface cluster (III) (Figure 3b). Significant differences between pairwise clusters were obtained using ANOSIM ($P < 0.05$). Clusters I and II were characterized by high aromatic compound contents (37.69–94.99%), while cluster III was characterized by a high fatty acid content (27.14–78.81%) (Figure 3a). Alkane/alkene compounds were also relatively abundant in the shelf-basin surface POM (0.45–13.33%).

3.2. Bacterial Community Structure

A total of 1 634 511 reads from the three size fractions of bacterial communities passed the quality control pipeline filters (supporting information Table S1); all libraries were divided into heterotrophic bacterial

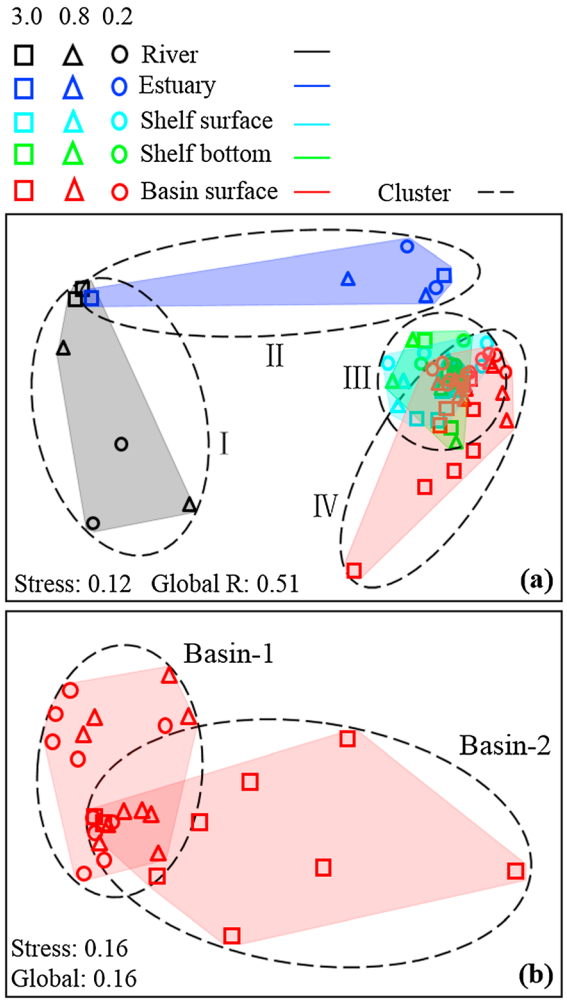

Figure 4. Nonmetric multidimensional scaling (NMDS) ordination based on Bray-Curtis similarities between heterotrophic bacterial (noncyanobacterial) communities ((a) all communities; (b) communities from basin surface). Each square (size fraction of >3 μm), triangle (0.8–3 μm), or circle (0.2–0.8 μm) represents an individual sample. Roman numerals in the NMDS charts represent cluster serial number.

and cyanobacterial subdata sets for downstream analyses. Diversity analysis showed quite variable diversity indices along the particle density gradient from freshwater to the sea basin. The highest diversities of heterotrophic bacterial communities occurred in the shelf region, followed by the sea basin; no distinct differences were observed between the different size fractions. In contrast, the highest diversities of cyanobacterial communities occurred in the freshwater region and gradually decreased in a seaward direction (supporting information Figure S2). However, the heterotrophic bacterial communities from 0.8–3 and >3 μm size fractions seemed to have higher diversities than those of the 0.2–0.8 μm communities in the freshwater and estuary regions (supporting information Figure S2), where the suspended particles were more abundant (Figure 1b), although statistical tests failed because of the small sample size. This might be explained by microenvironmental heterogeneity in particles resulting in higher heterogeneity in the taxonomic composition of the particle-attached bacterial community. In addition, the high diversity in sources of particulate matter in riverine and estuarine environments might contribute to the greater diversity of particle-attached heterotrophic bacteria observed.

Spatial variation in the bacterial community structure was analyzed based on two-dimensional NMDS ordination. All heterotrophic bacterial communities from the three size fractions were separated into four clusters along the particle density gradient from freshwater to the sea basin: freshwater cluster (I); estuary cluster (II); shelf surface–bottom cluster (III); and basin surface cluster (IV) (Figure 4a). Significant differences between pairwise clusters were obtained using ANOSIM ($P < 0.05$). No statistically significant differences were observed between different size fractions within each cluster, except for the basin cluster, in which the samples separated into two subclusters of the >3 μm fraction and the smaller size fractions (0.2–0.8 and 0.8–3 μm) (ANOSIM, $P < 0.05$; Figure 4b). SIMPER analysis revealed that Cluster I was characterized by high relative abundances of *Actinobacteria*, *Burkholderiales*, and *Rhizobiales*, Cluster II was characterized by high relative abundances of *Actinobacteria*, SAR11, and *Rhodobacteraceae*, while Clusters III and IV were characterized by high relative abundances of SAR11 (supporting information Table S2 and Figure S3).

3.3. Relationship Between Biochemical Properties of Particles and Bacterial Community Structure

CCA analyses were performed to further characterize variations in bacterial communities under the constraint of POM parameters. POC and PON concentration, $\delta^{13}C$, $\delta^{15}N$, C/N ratio, and total Chl *a* concentration, as well as basic hydrological parameters (temperature, salinity, and depth) and DOC concentration

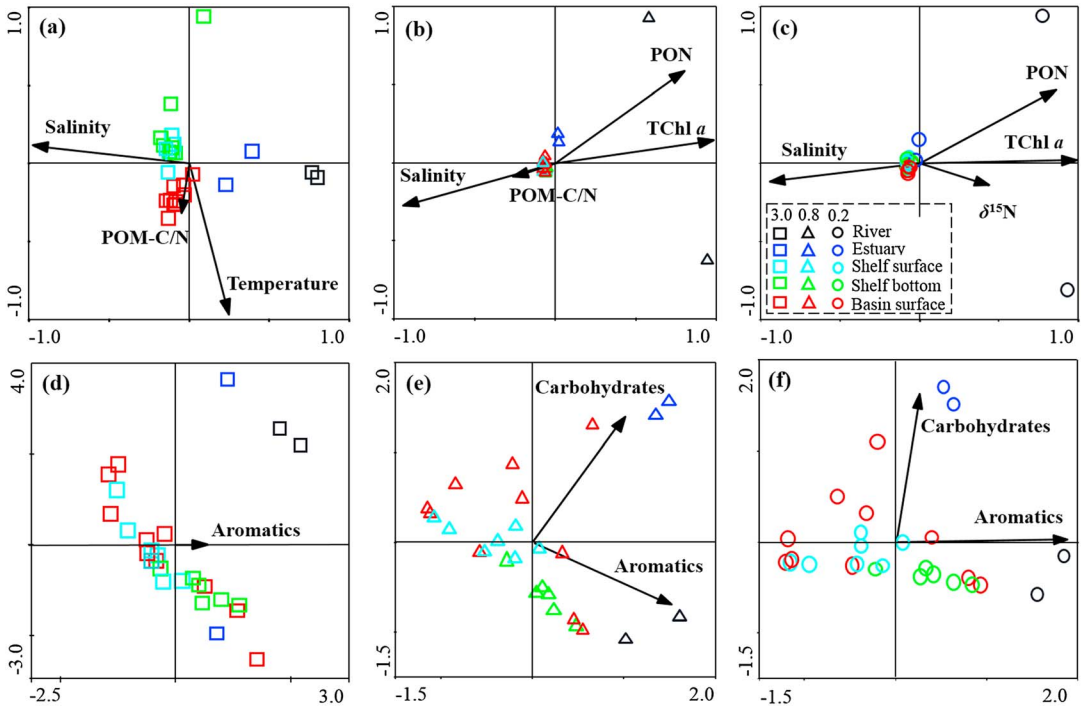

Figure 5. (a–f) Canonical correspondence analysis (CCA) in different size fractions. Each square (size fraction of > 3 μm), triangle (0.8–3 μm), or circle (0.2–0.8 μm) represents an individual sample. Vectors in the CCA charts represent statistically significant environmental variables (Figures 5a–5c) and POM chemical composition (Figures 5d–5f) explaining the observed patterns ($P < 0.05$).

(river, 179.91–194.86 μmol L^{-1}; estuary, 84.33–92.47 μmol L^{-1}; shelf, 68.30–80.57 μmol L^{-1}; basin, 65.41–74.9 μmol L^{-1}), were included in the stepwise procedure "forward selection" as candidates. Salinity, temperature, and the POM-C/N ratio were the most statistically significant variables ($P < 0.05$), partially explaining (approximately 24% of the total variance) the pattern of the heterotrophic bacterial community composition in the >3 μm size fraction (Figure 5a). Salinity, as a main factor discriminating different water masses, was also involved in the best combination of explanatory variables ($P < 0.05$) for the heterotrophic bacterial community in the other two size fractions. In addition, PON, total Chl *a* concentration, and POM-C/N ratio or POM-δ^{15}N, as the statistically significant particulate parameters ($P < 0.05$), were partially responsible for the spatial community variability in the 0.8–3 and 0.2–0.8 μm size fractions (approximately 38% and 37% of the total variance, respectively; Figures 5b and 5c). It is interesting to note that more POM parameters (three versus one) significantly explained more variance (37–38% versus 24%) in the free-living, rather than the particle-attached, bacterial community composition.

The CCA models revealed that the POM chemical compositions explained approximately 8, 14, and 14% of the total variance in the heterotrophic bacterial community composition in the >3, 0.8–3, and 0.2–0.8 μm size fractions, respectively. Aromatic content significantly ($P < 0.01$) explained the pattern of heterotrophic bacterial community composition in all three size fractions. In addition, carbohydrate content was related to community composition in the 0.8–3 and 0.2–0.8 μm size fractions (Figures 5d, 5e, and 5f). Carbohydrates in POM are mainly produced by phytoplankton in the coastal SCS and its basin [*Chen et al*., 1999]; the high carbohydrate contents in the freshwater and estuary samples were from both phytoplankton and terrestrial sources [*He et al*., 2010]. Carbohydrates in POM have high decay constants [*Benner and Amon*, 2014]. The relatively rapid turnover of the combined forms of carbohydrates in diverse marine environments has been well documented [*Davis and Benner*, 2007; *Steen et al*., 2008]. In addition, carbohydrate was lost from the particulate matter much faster than the other particulate organic constituents such as protein [*Handa and Yanagi*, 1969] and thus was a major source of the DOC throughout the surface ocean [*Biersmith and Benner*, 1998], which would impact the community composition of free-living heterotrophic bacteria. Aromatic compounds in POM are another important component of organic matter in the marginal seas by terrigenous input

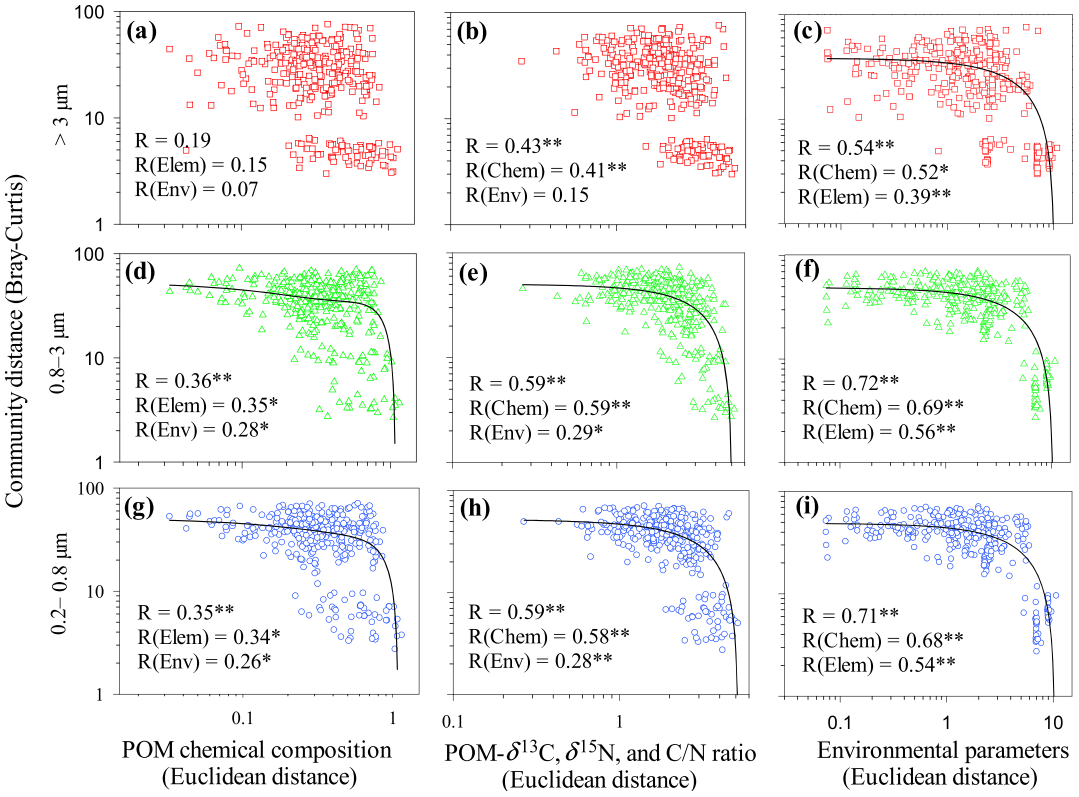

Figure 6. Correlations between bacterial community composition and POM chemical composition, POM elementary composition (δ^{13}C, δ^{15}N, and C/N ratio), or environmental parameters distance between samples. Pearson correlation coefficient (*R*) values are shown for regular (first value) and partial Mantel (second and third) tests. The *P* values were calculated using the distribution of the Mantel test statistics estimated from 999 permutations. *$P < 0.05$; **$P < 0.01$. Matrix of POM chemical composition was calculated according to the six types of compounds: aromatics, fatty acids, alkanes/alkenes, carbohydrates, phenols, and N compounds. Matrix of environmental parameters included POC, PON, total Chl *a*, DOC concentration, and the basic hydrological parameters (temperature, salinity, and depth).

[*Yang*, 2000]. Their influence on bacterial communities as carbon substrates has been reported in previous studies [*Carmona et al.*, 2009; *Wang et al.*, 2011]. Additionally, aromatic compounds could be produced by bacterial transformation [*Rossel et al.*, 2013; *Agarwal et al.*, 2014]. These results suggested that POM chemical composition significantly influenced particle-attached and free-living bacterial communities probably through direct substrate respiration and mechanical disaggregation [*Collins et al.*, 2015] or enzymatic solubilization [*Weston and Joye*, 2005; *Azam and Malfatti*, 2007; *Komada et al.*, 2012] of POM into the DOC pool. The latter might be the strongest effect of those identified, as POM chemical composition explained nearly one-fold higher variance (14% versus 8%) in free-living than particle-attached bacterial community composition.

Mantel and partial Mantel tests between matrices further demonstrated that the POM chemical composition and elemental composition were more strongly related to the heterotrophic bacterial community in the small size fractions (0.8–3 and 0.2–0.8 μm) with higher correlation coefficients than those of the >3 μm size fraction (Figure 6). No correlation was found between the POM chemical composition and community composition in the >3 μm size fraction (Figure 6a). In addition, the partial Mantel tests were insignificant between the heterotrophic bacterial community in the >3 μm size fraction and POM elemental composition, controlling for the effects of the environmental parameters matrix (Figure 6b). The above correlations for all samples in the SCS were contributed by the river, estuary, and shelf samples along sharp physical and chemical gradients with higher correlation coefficients (supporting information Figure S4). Strong correlations between environmental parameters and the size-fractionated heterotrophic bacterial communities were always observed (Figures 6c, 6f, and 6i). It seems possible that the observed close link between particulate chemical/elemental compositions and free-living bacterial community composition was because of their

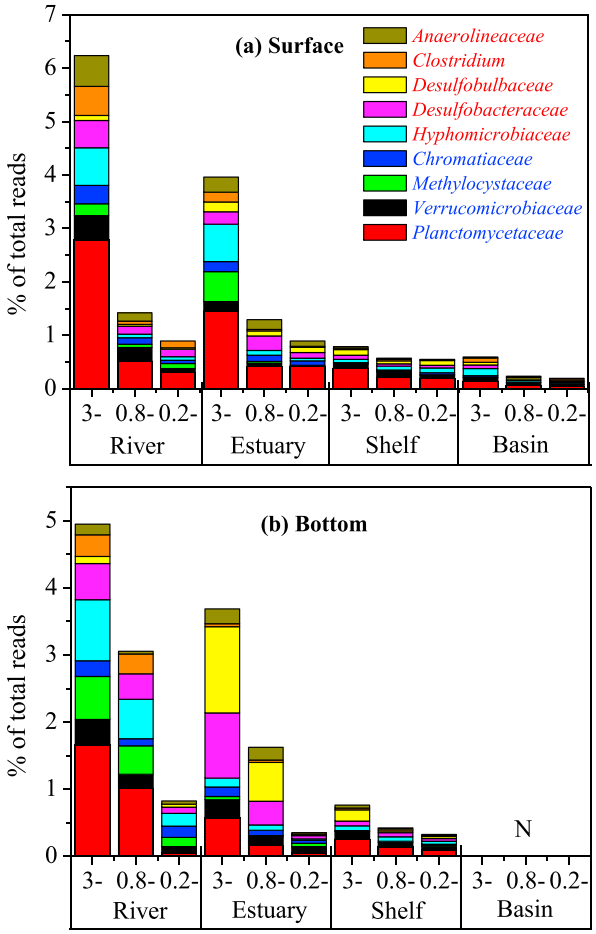

Figure 7. Distribution of anaerobic bacteria or bacteria preferring low-oxygen environments among the three size fractions of >3, 0.8–3, and 0.2–0.8 μm in the (a) surface and (b) bottom waters of the river, estuary, shelf, and basin. Values indicate means. Taxa shown in red and blue lettering are characterized as strict and facultative anaerobes, respectively. N indicates no samples.

covariation along environmental gradients. However, partial Mantel tests controlling for the effects of the matrix of environmental parameters further confirmed the significant correlation between them (Figures 6d, 6e, 6g, and 6h). As marine hotspots of bacterial growth, it has been reported that the exponential decay constant of POC was about 1.8–8.6-fold higher than that for DOC [*Hama et al*., 2004]. However, a recent study suggested that particle material was transferred to the water column by various biological processes and mechanical disaggregation nearly 3.5 times as fast as it was directly respired [*Collins et al*., 2015]. Hence, the release of labile or semilabile DOC from particles would significantly contribute to the bioavailability of DOC, which is an important substrate source for free-living bacterial populations.

3.4. Possible Role of Particle Microniche Properties in Shaping Particle-Attached Community Structure

The results of this study were inconsistent with the hypothesis that particle compositions have a stronger influence on particle-attached than free-living bacterial community composition. It was surprising to find that the composition of POM did not appear to have the same influence on the particle-attached bacteria. We further speculate that the particle microniche properties, rather than chemical composition, might have shaped the corresponding particle-attached bacterial community structure. An interesting finding is that anaerobic bacteria and those taxa preferring low-oxygen conditions were the most abundant in the >3 μm size fraction, followed by the 0.8–3 μm fraction (Figure 7). For instance, *Anaerolineaceae* [*Smith et al*., 2013], *Clostridium* [*Shimizu et al*., 2002], *Desulfobulbaceae, Desulfobacteraceae* [*Smith et al*., 2013], *Hyphomicrobiaceae* [*Stackebrandt*, 2004], *Chromatiaceae* [*Smith et al*., 2013], *Methylocystaceae* [*Dedysh*, 2011], *Verrucomicrobiaceae* [*Yoon et al*., 2008], and *Planctomycetaceae* [*Fuchsman et al*., 2012] were enriched in particle-attached communities, particularly in the river and estuary and in bottom waters, where suspended POM concentrations were very high. This finding suggested that there are low-oxygen microzones in particles [*Crump et al*., 1998; *Smith et al*., 2013; *Fontanez et al*.,2015]. An earlier study suggested that bacteria adhering onto a particle surface created oxygen-depleting microzones through physiological respiration [*Alldredge and Cohen*, 1987]. Particulate micropore fine structures might function as reaction centers for redox reactions in particles [*Liberti*, 1970; *Wang et al*., 2012]. In contrast, it was reported that in oxygenated water columns, oxygen could be unlimited at the aggregate-water interface by mass transfer and solute exchange processes [*Simon et al*., 2002]. Additionally, it was suggested that anoxic microniches might occur within large aggregates (≥1 mm), whereas in smaller aggregates (<1 to ≥0.1 mm), this only arises when ambient oxygen concentrations are ≤25 μM [*Klawonn et al*., 2015]. Hypoxia in the upper reaches of the Pearl River Estuary has been demonstrated

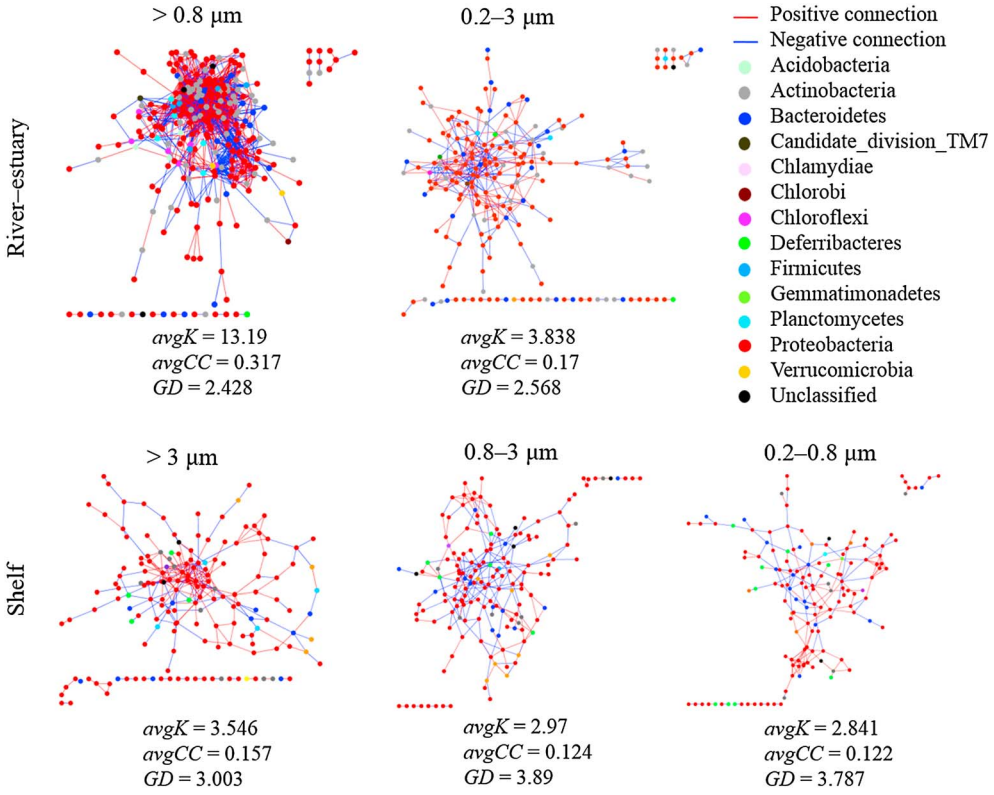

Figure 8. Network interactions of OTUs (organic layout) in the size-fractionated communities from the freshwater-estuary and shelf waters. Each line connects two OTUs. A blue line indicates a positive interaction between two individual nodes suggesting mutualism or cooperation, while a red line indicates a negative interaction suggesting predation or competition. Colors of the nodes indicate different major phyla. *AvgK*, *avgCC*, and *GD* are network topological indexes. Please refer to supporting information Tables S3 and S4 for the complete network indexes. *avgK*, average connectivity, higher *avgK* means a more complex network; *avgCC*, average clustering coefficient, it is used to measure the extent of module structure present in a network (i.e., the degree to which nodes in a graph tend to cluster together); *GD*, average geodesic distance, a small GD means all the nodes in the network are close together [*Deng et al*., 2012].

based on multiple-year observations [*He et al*., 2014]. It is also possible that the particles came from anoxic terrestrial environments and/or sediments, resulting in more abundant anaerobic bacteria associated with particles. Altogether, the present results imply that particle microniches, such as low-oxygen microzones in particles larger than 3 μm, might be important in shaping the corresponding particle-attached bacterial community structure.

Further evidence was provided by community network models. Based on the spatial structure of the bacterial community, three large clusters of heterotrophic bacterial communities corresponding to freshwater-estuary, shelf, and basin regions (Figure 4a: clusters I + II, III, and IV) were used for network analysis. The fractions of >3 and 0.8–3 μm were put together and 0.8–3 and 0.2–0.8 μm were put together for the freshwater-estuary region because the sample number must be ≥8 for network analysis. All curves of network connectivity fitted with the power-law model ($R^2 > 0.7$). Substantial differences were observed in terms of network size and structure among the size-fractionated heterotrophic bacterial communities in freshwater-estuary and shelf regions (Figure 8; supporting information Tables S3 and S4). The larger size fractions (>3 μm in shelf and >0.8 μm in freshwater-estuary waters) displayed the highest average connectivity, smallest average geodesic distance, and highest average clustering coefficient (Figure 8; supporting information Tables S3 and S4), suggesting tighter interactions [*Deng et al*., 2012] within particle-attached than free-living bacterial communities. In particles, a relatively confined space means that particle-attached bacteria are physically closer to their cooperators or competitors, facilitating metabolic cooperation, and genetic exchanges [*Grossart et al*., 2003; *Zhang et al*., 2014b; *Dang and Lovell*, 2016]. This further suggests that particulate microniches might play a role in shaping particle-attached bacterial community structure.

4. Conclusions

We report for the first time POM chemical compositions along the particle density gradient from freshwater to the sea basin in the SCS and link biochemical properties of particles to particle-attached and free-living bacterial communities to reveal how particulate properties shape bacterial community structure. There were distinct differences in POM isotopic composition, C/N ratio, chemical composition, and bacterial community composition among the freshwater, estuary, shelf, and sea basin regions. Spatial variations based on cluster analysis in bacterial communities and particulate chemical composition were generally consistent along the particle density gradient from freshwater to the sea basin. However, a correlation analysis between the biochemical properties of particles and bacterial community structure revealed that POM compositions were more strongly related to free-living rather than particle-attached bacterial communities. It is noteworthy that anaerobic bacteria were more abundant and those taxa preferring anoxic conditions comprised a larger size fraction of the particle-attached than the free-living bacterial community. This finding suggested that there might be low-oxygen microzones favoring their colonization in large-size particles. In addition, tighter interactions within the particle-attached than free-living communities suggested that a relatively confined space in particles is more favorable for interactions within the community. Therefore, particle microniches properties, rather than chemical composition, have shaped the corresponding particle-attached bacterial community structure. In contrast, particulate elemental and chemical compositions had stronger links to bacterial communities in the smaller size fractions than the larger ones, as indicated by the CCA analysis and Mantel tests, implying that the release of labile or semilabile DOC from particles would contribute to the bioavailability of DOC for free-living bacterial populations.

Acknowledgments

The authors would like to thank Meilin Wu, Chief Scientist, NSFC SCS cruise, for providing the sampling opportunity and temperature and salinity data, Wupeng Xiao for his assistance with Chl *a* concentration measurements, Rui Wang for her assistance with DOC concentration measurements, and our colleagues who helped with sampling. In the preparation of the manuscript, Shuh-Ji Kao provided valuable comments and suggestions. This research was supported by the national key research programs 2016YFA0601400 and 2013CB955700, the NSFC projects 41422603 , 41676125 and 91428308, and the SOA project GASI-03-01-02-03. Supporting information can be found on the website. The authors declare no conflict of interests. All data are available upon request from Y.Z. (yaozhang@xmu.edu). Yao Zhang and Wei Xiao contributed equally to this work.

References

Agarwal, V., A. A. El Gamal, K. Yamanaka, D. Poth, R. D. Kersten, M. Schorn, E. E. Allen, and B. S. Moore (2014), Biosynthesis of polybrominated aromatic organic compounds by marine bacteria, *Nat. Chem. Boil.*, *10*(8), 640–647.

Alldredge, A. L., and Y. Cohen (1987), Can microscale chemical patches persist in the sea? Microelectrode study of marine snow, fecal pellets, *Science*, *235*(4789), 689–691.

Azam, F., and R. A. Long (2001), Oceanography: Sea snow microcosms, *Nature*, *414*(6863), 495–498.

Azam, F., and F. Malfatti (2007), Microbial structuring of marine ecosystems, *Nat. Rev. Microbiol.*, *5*(10), 782–791.

Bascompte, J. (2007), Networks in ecology, *Basic Appl. Ecol.*, *8*(6), 485–490.

Benner, R., and R. M. Amon (2014), The Size-Reactivity Continuum of Major Bioelements in the Ocean, *Ann. Rev. Mar. Sci.*, *7*(1), 185–205.

Biersmith, A., and R. Benner (1998), Carbohydrates in phytoplankton and freshly produced dissolved organic matter, *Mar. Chem.*, *63*(1), 131–144.

Carlson, C. A., R. Morris, R. Parsons, A. H. Treusch, S. J. Giovannoni, and K. Vergin (2008), Seasonal dynamics of SAR11 populations in the euphotic and mesopelagic zones of the northwestern Sargasso Sea, *ISME J.*, *3*(3), 283–295.

Carmona, M., M. T. Zamarro, B. Blázquez, G. Durante-Rodríguez, J. F. Juárez, J. A. Valderrama, M. J. Barragán, J. L. García, and E. Díaz (2009), Anaerobic catabolism of aromatic compounds: A genetic and genomic view, *Microbiol. Mol. Biol. Rev.*, *73*(1), 71–133.

Chen, J., M. Wiesner, H. Wong, L. Zheng, L. Xu, and S. Zheng (1999), Vertical changes of POC flux and indicators of early degradation of organic matter in the South China Sea, *Sci. China, Ser. D*, *42*(2), 120–128.

Clarke, K., and R. Warwick (1994), *Change in Marine Communities: An Approach to Statistical Analysis and Interpretation*, Natural Environment Research Council, Swindon, U. K.

Çoban-Yıldız, Y., M. A. Altabet, A. Yılmaz, and S. Tuğrul (2006a), Carbon and nitrogen isotopic ratios of suspended particulate organic matter (SPOM) in the Black Sea water column, *Deep Sea Res., Part II*, *53*(17), 1875–1892.

Çoban-Yıldız, Y., D. Fabbri, V. Baravelli, I. Vassura, A. Yılmaz, S. Tuğrul, and E. Eker-Develi (2006b), Analytical pyrolysis of suspended particulate organic matter from the Black Sea water column, *Deep Sea Res., Part II*, *53*(17), 1856–1874.

Collins, J. R., B. R. Edwards, K. Thamatrakoln, J. E. Ossolinski, G. R. DiTullio, K. D. Bidle, S. C. Doney, and B. A. Van Mooy (2015), The multiple fates of sinking particles in the North Atlantic Ocean, *Global Biogeochem. Cycles*, *29*, 1471–1494, doi:10.1002/2014GB005037.

Conan, P., M. Søndergaard, T. Kragh, F. Thingstad, M. Pujo-Pay, P. J. B. Williams, S. Markager, G. Cauwet, N. H. Borch, and D. Evans (2007), Partitioning of organic production in marine plankton communities: The effects of inorganic nutrient ratios and community composition on new dissolved organic matter, *Limnol. Oceanogr.*, *52*(2), 753–765.

Crump, B. C., J. A. Baross, and C. A. Simenstad (1998), Dominance of particle-attached bacteria in the Columbia River estuary, USA, *Aquat. Microb. Ecol.*, *14*(1), 7–18.

Crump, B. C., E. V. Armbrust, and J. A. Baross (1999), Phylogenetic analysis of particle-attached and free-living bacterial communities in the Columbia river, its estuary, and the adjacent coastal ocean, *Appl. Environ. Microbiol.*, *65*(7), 3192–3204.

D'Ambrosio, L., K. Ziervogel, B. MacGregor, A. Teske, and C. Arnosti (2014), Composition and enzymatic function of particle-associated and free-living bacteria: A coastal/offshore comparison, *ISME J.*, *8*, 2167–2179.

Dang, H., and C. R. Lovell (2016), Microbial surface colonization and biofilm development in marine environments, *Microbiol. Mol. Biol. Rev.*, *80*(1), 91–138.

Davis, J., and R. Benner (2007), Quantitative estimates of labile and semi-labile dissolved organic carbon in the western Arctic Ocean: A molecular approach, *Limnol. Oceanogr.*, *52*(6), 2434–2444.

Dedysh, S. N. (2011), Cultivating uncultured bacteria from northern wetlands: knowledge gained and remaining gaps, *Front. Microbiol.*, *2*, 184.

Delong, E. F., D. G. Franks, and A. L. Alldredge (1993), Phylogenetic diversity of aggregate-attached vs. free-living marine bacterial assemblages, *Limnol. Oceanogr.*, *38*(5), 924–934.

Deng, Y., Y.-H. Jiang, Y. Yang, Z. He, F. Luo, and J. Zhou (2012), Molecular ecological network analyses, *BMC Bioinf.*, *13*(1), 113.
Edwards, B. R., K. D. Bidle, and B. A. S. van Mooy (2015), Dose-dependent regulation of microbial activity on sinking particles by polyunsaturated aldehydes: Implications for the carbon cycle, *Proc. Natl. Acad. Sci. U.S.A.*, *112*(19), 5909–5914.
Fontanez, K. M., J. M. Eppley, T. J. Samo, D. M. Karl, and E. F. DeLong (2015), Microbial community structure and function on sinking particles in the North Pacific Subtropical Gyre, *Front. Microbiol.*, *6*, 469.
Fuchsman, C. A., J. T. Staley, B. B. Oakley, J. B. Kirkpatrick, and J. W. Murray (2012), Free-living and aggregate-associated Planctomycetes in the Black Sea, *FEMS Microbiol. Ecol.*, *80*(2), 402–416.
Fuhrman, J. A., J. A. Steele, I. Hewson, M. S. Schwalbach, M. V. Brown, J. L. Green, and J. H. Brown (2008), A latitudinal diversity gradient in planktonic marine bacteria, *Proc. Natl. Acad. Sci. U.S.A.*, *105*(22), 7774–7778.
Ganesh, S., D. J. Parris, E. F. DeLong, and F. J. Stewart (2014), Metagenomic analysis of size-fractionated picoplankton in a marine oxygen minimum zone, *ISME J.*, *8*(1), 187–211.
Geider, R., and J. La Roche (2002), Redfield revisited: Variability of C: N: P in marine microalgae and its biochemical basis, *Eur. J. Phycol.*, *37*(1), 1–17.
Ghiglione, J. F., G. Mevel, M. Pujo-Pay, L. Mousseau, P. Lebaron, and M. Goutx (2007), Diel and seasonal variations in abundance, activity, and community structure of particle-attached and free-living bacteria in NW Mediterranean Sea, *Microb. Ecol.*, *54*(2), 217–231.
Grossart, H.-P. (2010), Ecological consequences of bacterioplankton lifestyles: Changes in concepts are needed, *Environ. Microbiol. Rep.*, *2*(6), 706–714.
Grossart, H.-P., T. Kiørboe, K. Tang, and H. Ploug (2003), Bacterial colonization of particles: Growth and interactions, *Appl. Environ. Microbiol.*, *69*(6), 3500–3509.
Hama, T., K. Yanagi, and J. Hama (2004), Decrease in molecular weight of photosynthetic products of marine phytoplankton during early diagenesis, *Limnol. Oceanogr.*, *49*(2), 471–481.
Handa, N., and K. Yanagi (1969), Studies on water-extractable carbohydrates of the particulate matter from the northwest Pacific Ocean, *Mar. Biol.*, *4*(3), 197–207.
He, B., M. Dai, W. Huang, Q. Liu, H. Chen, and L. Xu (2010), Sources and accumulation of organic carbon in the Pearl River Estuary surface sediment as indicated by elemental, stable carbon isotopic, and carbohydrate compositions, *Biogeosciences*, *7*, 3343–3362.
He, B., M. Dai, W. Zhai, X. Guo, and L. Wang (2014), Hypoxia in the upper reaches of the Pearl River Estuary and its maintenance mechanisms: A synthesis based on multiple year observations during 2000–2008, *Mar. Chem.*, *167*, 13–24.
Huang, B., J. Hu, H. Xu, Z. Cao, and D. Wang (2010), Phytoplankton community at warm eddies in the northern South China Sea in winter 2003/2004, *Deep Sea Res., Part II*, *57*(19), 1792–1798.
Jiao, N., G. J. Herndl, D. A. Hansell, R. Benner, G. Kattner, S. W. Wilhelm, D. L. Kirchman, M. G. Weinbauer, T. Luo, and F. Chen (2010), Microbial production of recalcitrant dissolved organic matter: Long-term carbon storage in the global ocean, *Nat. Rev. Microbiol.*, *8*(8), 593–599.
Jiao, N., et al. (2014), Mechanisms of microbial carbon sequestration in the ocean—Future research directions, *Biogeosciences*, *11*(19), 5285–5306.
Kao, S.-J., J.-Y. Terence Yang, K.-K. Liu, M. Dai, W.-C. Chou, H.-L. Lin, and H. Ren (2012), Isotope constraints on particulate nitrogen source and dynamics in the upper water column of the oligotrophic South China Sea, *Global Biogeochem. Cycles*, *26*, GB2033, doi:10.1029/2011GB004091.
Klawonn, I., S. Bonaglia, V. Brüchert, and H. Ploug (2015), Aerobic and anaerobic nitrogen transformation processes in N_2-fixing cyanobacterial aggregates, *ISME J.*, *9*(6), 1456–1466.
Komada, T., J. A. Polly, and L. Johnson (2012), Transformations of carbon in anoxic marine sediments: Implications from $\Delta^{14}C$ and $\delta^{13}C$ signatures, *Limnol. Oceanogr.*, *57*(2), 567–581.
Kozich, J. J., S. L. Westcott, N. T. Baxter, S. K. Highlander, and P. D. Schloss (2013), Development of a dual-index sequencing strategy and curation pipeline for analyzing amplicon sequence data on the MiSeq Illumina sequencing platform, *Appl. Environ. Microbiol.*, *79*(17), 5112–5120.
Kruskal, J. B. (1964), Multidimensional scaling by optimizing goodness of fit to a nonmetric hypothesis, *Psychometrika*, *29*(1), 1–27.
Kumar, S., J. C. Finlay, and R. W. Sterner (2011), Isotopic composition of nitrogen in suspended particulate matter of Lake Superior: Implications for nutrient cycling and organic matter transformation, *Biogeochemistry*, *103*(1), 1–14.
Liberti, A. (1970), The nature of particulate matter, *Pure Appl. Chem.*, *24*(4), 631–642.
Magoč, T., and S. L. Salzberg (2011), FLASH: Fast length adjustment of short reads to improve genome assemblies, *Bioinformatics*, *27*(21), 2957–2963.
Massana, R., E. F. DeLong, and C. Pedrós-Alió (2000), A few cosmopolitan phylotypes dominate planktonic archaeal assemblages in widely different oceanic provinces, *Appl. Environ. Microbiol.*, *66*(5), 1777–1787.
Montoya, J. M., S. L. Pimm, and R. V. Solé (2006), Ecological networks and their fragility, *Nature*, *442*(7100), 259–264.
Ning, X., F. Chai, H. Xue, Y. Cai, C. Liu, and J. Shi (2004), Physical-biological oceanographic coupling influencing phytoplankton and primary production in the South China Sea, *J. Geophys. Res.*, *109*, C10005, doi:10.1029/2004JC002365.
Pennock, J. R., D. J. Velinsky, J. M. Ludlam, J. H. Sharp, and M. L. Fogel (1996), Isotopic fractionation of ammonium and nitrate during uptake by Skeletonema costatum: Implications for $\delta^{15}N$ dynamics under bloom conditions, *Limnol. Oceanogr.*, *41*(3), 451–459.
Rossel, P. E., A. V. Vähätalo, M. Witt, and T. Dittmar (2013), Molecular composition of dissolved organic matter from a wetland plant (Juncus effusus) after photochemical and microbial decomposition (1.25 yr): Common features with deep sea dissolved organic matter, *Org. Geochem.*, *60*, 62–71.
Sherwood, C., J. Creager, E. Roy, G. Gelfenbaum, and T. Dempsey (1984), *Sedimentary Processes and Environments in the Columbia River Estuary*, Columbia River Estuary Data Development Program, Portland, Oreg.
Shimizu, T., K. Ohtani, H. Hirakawa, K. Ohshima, A. Yamashita, T. Shiba, N. Ogasawara, M. Hattori, S. Kuhara, and H. Hayashi (2002), Complete genome sequence of Clostridium perfringens, an anaerobic flesh-eater, *Proc. Natl. Acad. Sci. U.S.A.*, *99*(2), 996–1001.
Simon, H. M., M. W. Smith, and L. Herfort (2014), Metagenomic insights into particles and their associated microbiota in a coastal margin ecosystem, *Front. Microbiol.*, *5*, 466.
Simon, M., H.-P. Grossart, B. Schweitzer, and H. Ploug (2002), Microbial ecology of organic aggregates in aquatic ecosystems, *Aquat. Microb. Ecol.*, *28*(2), 175–211.
Smith, M. W., L. Z. Allen, A. E. Allen, L. Herfort, and H. M. Simon (2013), Contrasting genomic properties of free-living and particle-attached microbial assemblages within a coastal ecosystem, *Front. Microbiol.*, *4*, 120.
Sogin, M. L., H. G. Morrison, J. A. Huber, D. M. Welch, S. M. Huse, P. R. Neal, J. M. Arrieta, and G. J. Herndl (2006), Microbial diversity in the deep sea and the underexplored "rare biosphere", *Proc. Natl. Acad. Sci. U.S.A.*, *103*, 12,115–12,120.

Stackebrandt, E. (2004), The phylogeny and classification of anaerobic bacteria, in Strict and Facultative Anaerobes. *Medical and Environmental Aspects,* 1–25.

Steen, A. D., L. J. Hamdan, and C. Arnosti (2008), Dynamics of dissolved carbohydrates in the Chesapeake Bay: Insights from enzyme activities, concentrations, and microbial metabolism, *Limnol. Oceanogr.*, *53*(3), 936–947.

Stocker, R. (2012), Marine microbes see a sea of gradients, *Science*, *338*(6107), 628–633.

Strom, S. L., R. Benner, S. Ziegler, and M. J. Dagg (1997), Planktonic grazers are a potentially important source of marine dissolved organic carbon, *Limnol. Oceanogr.*, *42*(6), 1364–1374.

Ter Braak, C. J. (1986), Canonical correspondence analysis: A new eigenvector technique for multivariate direct gradient analysis, *Ecology*, *67*, 1167–1179.

Ter Braak, C. J. (1989), CANOCO—An extension of DECORANA to analyze species-environment relationships, *Hydrobiologia*, *184*, 169–170.

Uitz, J. U., Y. Huot, F. Bruyant, M. Babin, and H. Claustre (2008), Relating phytoplankton photophysiological properties to community structure on large scales, *Limnol. Oceanogr.*, *53*(2), 614–630.

Wang, D. W., F. Li, L. C. Yin, X. Lu, Z. G. Chen, I. R. Gentle, G. Q. M. Lu, and H. M. Cheng (2012), Nitrogen-doped carbon monolith for alkaline supercapacitors and understanding nitrogen-induced redox transitions, *Chem. Eur. J.*, *18*(17), 5345–5351.

Wang, Y., J. Yang, O. O. Lee, S. Dash, S. C. Lau, A. Al-Suwailem, T. Y. Wong, A. Danchin, and P.-Y. Qian (2011), Hydrothermally generated aromatic compounds are consumed by bacteria colonizing in Atlantis II Deep of the Red Sea, *ISME J.*, *5*(10), 1652–1659.

Weston, N. B., and S. B. Joye (2005), Temperature-driven decoupling of key phases of organic matter degradation in marine sediments, *Proc. Natl. Acad. Sci. U.S.A.*, *102*(47), 17,036–17,040.

Wu, K., M. Dai, J. Chen, F. Meng, X. Li, Z. Liu, C. Du, and J. Gan (2015), Dissolved organic carbon in the South China Sea and its exchange with the Western Pacific Ocean, *Deep Sea Res., Part II*, *122*, 41–51.

Yang, G.-P. (2000), Polycyclic aromatic hydrocarbons in the sediments of the South China Sea, *Environ. Pollut.*, *108*(2), 163–171.

Yoon, J., Y. Matsuo, K. Adachi, M. Nozawa, S. Matsuda, H. Kasai, and A. Yokota (2008), Description of Persicirhabdus sediminis gen. nov., sp. nov., Roseibacillus ishigakijimensis gen. nov., sp. nov., Roseibacillus ponti sp. nov., Roseibacillus persicicus sp. nov., Luteolibacter pohnpeiensis gen. nov., sp. nov. and Luteolibacter algae sp. nov., six marine members of the phylum 'Verrucomicrobia', and emended descriptions of the class Verrucomicrobiae, the order Verrucomicrobiales and the family Verrucomicrobiaceae, *Int. J. Syst. Evol. Micr.*, *58*(4), 998–1007.

Zhang, R., B. Liu, S. C. Lau, J. S. Ki, and P. Y. Qian (2007), Particle-attached and free-living bacterial communities in a contrasting marine environment: Victoria Harbor, Hong Kong, *FEMS Microbiol. Ecol.*, *61*(3), 496–508.

Zhang, Y., X. Xie, N. Jiao, S.-Y. Hsiao, and S.-J. Kao (2014a), Diversity and distribution of amoA-type nitrifying and nirS-type denitrifying microbial communities in the Yangtze River estuary, *Biogeosciences*, *11*(8), 2131–2145.

Zhang, Y., Z. Zhao, M. Dai, N. Jiao, and G. J. Herndl (2014b), Drivers shaping the diversity and biogeography of total and active bacterial communities in the South China Sea, *Mol. Ecol.*, *23*(9), 2260–2274.

Zhang, Y., K. Kaiser, L. Li, D. Zhang, Y. Ran, and R. Benner (2014c), Sources, distributions, and early diagenesis of sedimentary organic matter in the Pearl River region of the South China Sea, *Mar. Chem.*, *158*, 39–48.

Zhao, H., D. Tang, and D. Wang (2009), Phytoplankton blooms near the Pearl River estuary induced by Typhoon Nuri, *J. Geophys. Res.*, *114*, C12027, doi:10.1016/j.jmarsys.2005.09.002.

Zhou, J., Y. Deng, F. Luo, Z. He, Q. Tu, and X. Zhi (2010), Functional molecular ecological networks, *MBio*, *1*(4), e00169–00,110.